Published in Optics Communications **130**, Sep. 1996, pp. 272-278.

Anisotropic Unidirectional Operation of an Optically-Pumped $\mathrm{CH_3OH}$ Ring Laser

K. Matsushima[†], K. Hirata and T. Ariyasu
Department of Electrical Engineering, Kansai University

N. Sokabe
Department of Applied Physics, Osaka City University
Sugimoto 3-3-138, Osaka 558, Japan

Abstract

We report directional anisotropy of the outputs of an optically pumped far-infrared ring laser, which operates on 119 μm line of $\mathrm{CH_3OH}$, with special emphasis on the effect of Raman-type two-photon process on unidirectional operation. By use of a Doppler broadened 3-level system which allows coexistence of two counterpropagating far infrared (fir) fields as well as a pump field in the cavity, expression for the fir intensity determining equations is derived. Numerical calculation has been carried out to map the threshold contours on the parameter plane spanned by cavity and pump detuning frequencies. The output directionality is shown to be a direct consequence of the gain anisotropy due to two-photon process. Furthermore, it is also noted that how dynamic Stark effect modifies the threshold contours of the forward output.

1 Introduction

One of the unique aspects of operation of optically pumped far infrared ring lasers (OPFRL's) is unidirectional output. In ordinary ring gas lasers pumped incoherently (e.g., with electrical discharge), the velocity distribution of the excited atoms in the medium is Maxwellian. So far as the Doppler width is large compared with the homogeneous linewidth, the two radiation fields with the same frequency counterpropagating with each other in the cavity interact with the ensemble of atoms with different velocities. The two fields do not couple with the group of atoms

[†]E-mail: matsu@laser.ee.kansai-u.ac.jp

with the same velocity, except for the case with central cavity tuning at a low rotation rate of a ring cavity [1]. In case of OPFRL's, the velocity distribution of the active molecules optically pumped with an infrared field with an wavenumber of $\vec{K}_P$ is not described by Maxwellian distribution because of velocity selective excitation. With a pump frequency detuned from the absorption line center by Δ_P, the velocity distribution of the excited molecules is approximately limited within a narrow range of $2\gamma_P/|\vec{K}_P|$ around $\Delta_P/|\vec{K}_P|$, where γ_P denotes the homogeneous linewidth of the pump transition. As a result, the output directionality of OPFRL's is entirely different from that of discharge-pumped ring gas lasers. Ordinary ring gas lasers operate bidirectionally except for central cavity tuning at a low rotation rate of the cavity, while OPFRL's operate unidirectionally and its output direction changes depending on fir cavity [2] as well as on ir pump detunings [3].

Vilaseca and coworkers analyzed the output directionality of an OPFRL [4]. They, however, did not examine the stability of the stationary solutions for the fir outputs. By using a simplified model, we previously reported stability of the stationary solutions to the intensity determining equations of an OPFRL [3] and showed competition between two modes emitting in forward and backward directions plays an important role. However, Raman-type two-photon process, which presumably affects the output directionality of realistic OPFRL's [5], was neglected in Ref.[3].

In this paper, we report theoretical and experimental study of the effect of the two-photon process on the output directionality of an OPFRL operating on the 119 μm line of $\mathrm{CH_3OH}$. A closed form of an expression of gains for a Doppler broadened 3-level system including Raman-type two-photon process in the presence of two far infrared fields counterpropagating with each other was reported elsewhere [6]. We herein apply the expression of the gain reported in Ref.[6] to calculate the stable stationary fir output intensities.

The threshold condition maps the contours of the forward and backward fir outputs on the parameter plane spanned by cavity and pump detuning frequencies. The dependence of output direction of the OPFRL on pump frequency and vapor pressure will be discussed.

2 Experimental

Experimental setup for observing output directionality of an optically pumped far-infrared ring laser is shown in Fig. 1. The ring cavity is installed inside a vacuum vessel. The cavity consists of four Au-coated concave mirrors ($\mathrm{M_1} \sim \mathrm{M_4}$). The vacuum vessel was filled up with methanol vapor as a laser medium. Each of the three mirrors $\mathrm{M_2}$, $\mathrm{M_3}$ and $\mathrm{M_4}$ has a central coupling hole of 1.5mm in diameter. The infrared pump beam is led into the cavity through the hole on $\mathrm{M_2}$. The forward and backward outputs are coupled out of the cavity via the hole on mirrors $\mathrm{M_4}$ and $\mathrm{M_3}$, respectively. The pump source is a conventional $\mathrm{CO_2}$ laser which delivers a maximum output power of approximately 12 W on P(36) line of 9μm

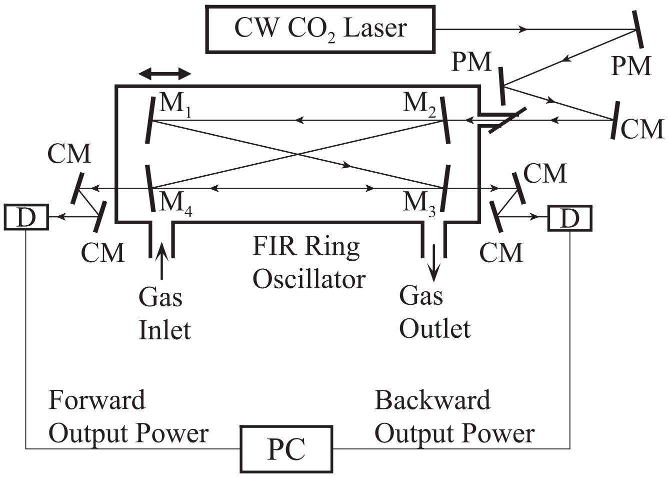

Fig. 1 Experimental setup for observing the forward and backward outputs of an optically pumped fir ring laser. CM: concave mirror, PM: plane mirror, D: pyroelectric detector.

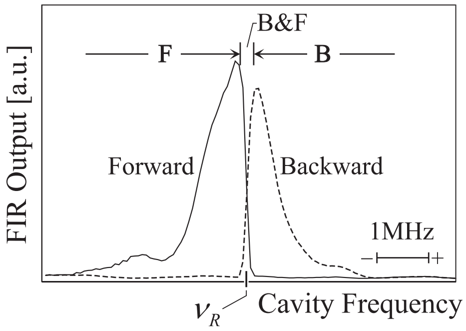

Fig. 2 A typical cavity tuning curve of 119 μm CH_3OH ring laser. The pump power was 11 W and the vapor pressure was 14 Pa. F: forward unidirectional, B: backward unidirectional, B&F: bi-directional.

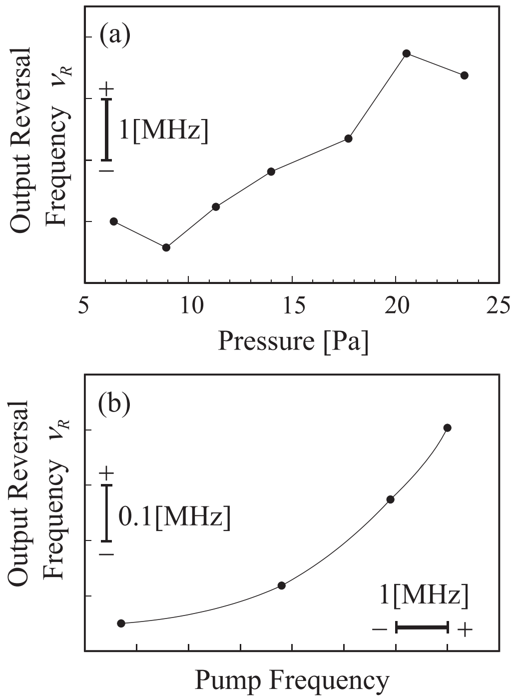

Fig. 3 Output reversal frequency vs $\mathrm{CH_3OH}$ vapor pressure (a) and pump frequency (b). The pump power was 12 W and the pump detuning was negative. The vapor pressure was 14 Pa in (b).

band (9P(36)).

A cavity tuning curve of the 119 μm line pumped with $\mathrm{CO_2}$ 9P(36) is shown in Fig. 2. The pump power is 11 W and pump detuning is negative. The OPFRL which nominally operates unidirectionally experiences reversal of its output direction at a particular cavity frequency as the cavity is tuned across the fir line center. The particular cavity frequency is hereafter referred to as the output reversal frequency ν_R.

The output reversal frequency ν_R changes depending on ir pump frequency as well as on vapor pressure of $\mathrm{CH_3OH}$. The frequency ν_R is plotted as a function of medium pressure in Fig. 3(a). The frequency ν_R tends to increase with vapor pressure. For a given negative pump detuning, the change in ν_R was approximately 3 MHz at most as the pressure was increased from 6 Pa to 24 Pa. The frequency ν_R as a function of pump frequency is shown in Fig. 3(b). A change in ν_R was approximately 0.35 MHz as the pump frequency was tuned over 6.3 MHz. It is noted in Fig. 3 that the OPFRL emits backward output for cavity frequencies above ν_R and forward one bellow ν_R.

A mode competition model [3] in which gain anisotropy due to two-photon process is ignored predicts that the reversal frequency ν_R corresponds exactly to

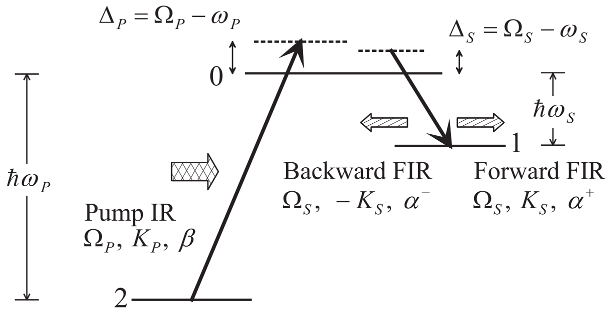

Fig. 4 A model for an optically pumped fir ring laser.

the center frequency of the fir transition, regardless of the operating condition. The change in ν_R with vapor pressure and pump frequency is a direct evidence of a gain anisotropy with respect to forward and backward directions.

3 Analysis

3.1 Theoretical model and intensity determining equations

A three level scheme for optically pumped fir lasers is shown in Fig. 4. The ir wave with a frequency Ω_P and a wavenumber of K_P pumps the 2-0 transition with Rabi frequency β. Two fir waves counterpropagating with each other couple with the 0-1 transition. An angular frequency and wavenumbers of the two fir waves are denoted by Ω_S and $\pm K_S$, respectively, and Rabi frequencies are denoted by $\alpha^{\pm}$. We refer to the fir wave co- and counter-propagating with the pump wave as the "forward" and "backward" fir waves, respectively. The positive sign is assigned to the forward wave while negative to the backward wave. Both the ir and fir transitions are assumed to be Doppler broadened.

In the level scheme of Fig. 4, the far-infrared coherence is given by

$$\rho_{01} \equiv \sigma_{01}^{+} \exp[-i(\Omega_S t - K_S z)] + \sigma_{01}^{-} \exp[-i(\Omega_S t + K_S z)],$$

where σ_{01}^{+} and σ_{01}^{-} are slowly varying amplitudes. By neglecting terms with higher-order spatial Fourier components of density matrix, $\exp(\pm inK_S z)$ $(n \geq 2)$, we have derived a closed form of expression for far-infrared susceptibility in rotating wave approximation and steady-state condition without using perturbation expansion [6]. The model describes cross saturation of fir gains and dynamic Stark effect as well as the basic spectroscopic feature such as two-photon transition that is inherent to the coupled transitions in 3-level system.

The equation of motion of the Rabi frequencies $\alpha^{\pm}$ are given as

$$\frac{d\alpha^{\pm}}{dt} = -\frac{\gamma_c \alpha^{\pm}}{2} - \frac{\mu_{01}^2 \Omega_S}{4\hbar\varepsilon_0} \mathrm{Im} \int_{-\infty}^{\infty} N_t \sigma_{01}^{\pm} dv, \tag{1}$$

where N_t and γ_c are the number density of molecules and the cavity decay constant, respectively. Substituting the expression for $\sigma_{01}^{\pm}$ given in Ref.[6] into eq.(1), one obtains

$$\begin{aligned}\frac{d|\alpha^{\pm}|^2}{d\tau} &= |\alpha^{\pm}|^2 \\ &\times \left[\eta_g \int_{-\infty}^{\infty} \mathrm{Im}\, \frac{A^{\mp}|\beta|^2(1-J_{11}) + [A^{\mp}C^{\pm} - B^{\mp}|\alpha^{\mp}|^2]J_{12}}{D[(1-J_{11})(1-J_{22}) - J_{12}J_{21}]} f(v)dv - 1\right],\end{aligned} \tag{2}$$

with

$$\eta_g \equiv \frac{\mu_{01}^2 \Omega_S N_t d^0}{2\hbar\varepsilon_0\gamma_c}, \tag{3}$$

where $\tau = t\gamma_c$, and dispersion of the medium is neglected. We have neglected the thermal population in the vibrationally excited state at room temperature, and denoted the thermal population difference between the states 2 and 0 by $N_t d^0$. Maxwellian velocity distribution function, $f(v) = (\sqrt{\pi}u)^{-1}\exp[-(v/u)^2]$, has been assumed for molecular velocity distribution. The definition of other symbols in Eq.(2) is given in Table I of Ref.[6]. Stable stationary fir intensities are obtained by integration of Eq.(2). Starting from a small initial value, we have calculated time development of $|\alpha^{\pm}|^2$ until they get stationary values. It is noted that the slowly varying amplitude $\sigma_{01}^{\pm}$ and variables $A^{\pm}$, $B^{\pm}$, $C^{\pm}$, D and J_{ij} in Eq.(2) are a function of molecular velocity v.

3.2 Input parameters

The calculation was made on 119 μm line of $\mathrm{CH_3OH}$ pumped with $\mathrm{CO_2}$ 9P(36). The parameters necessary for numerical calculation were taken from literature [7], except for η_g. For estimation of η_g, one needs the cavity decay constant γ_c. In this work, instead of evaluating γ_c, we have chosen the value of η_g so that calculated cavity tuning curve is in agreement with the observation. It is noted that η_g [s^{-1}] is proportional to N_t, i.e. vapor pressure. We have assumed that $\eta_g = 50 \times \gamma_0$.

3.3 Results of numerical calculation

The calculated threshold contours are plotted on Δ_P - Δ_S plane in Fig. 5 for different vapor pressures. Unidirectional forward output is expected at around cavity resonance ($\Delta_S \sim 0$) and resonant pump frequency ($\Delta_P \sim 0$) at pressures above 9 Pa. With an increase in vapor pressure, the area for unidirectional backward output on the Δ_P - Δ_S plane decreases and eventually disappears at pressures higher than 30 Pa. The area for unidirectional forward output decreases with decreasing vapor pressure and splitting is observed at pressures below 5 Pa. No forward output is expected on the whole Δ_P - Δ_S plane when the pressure is further decreased.

Note that in Fig. 3 the observed frequency ν_R refers to the cavity frequency which, in general, is different from the frequency of fir waves. Though dispersion

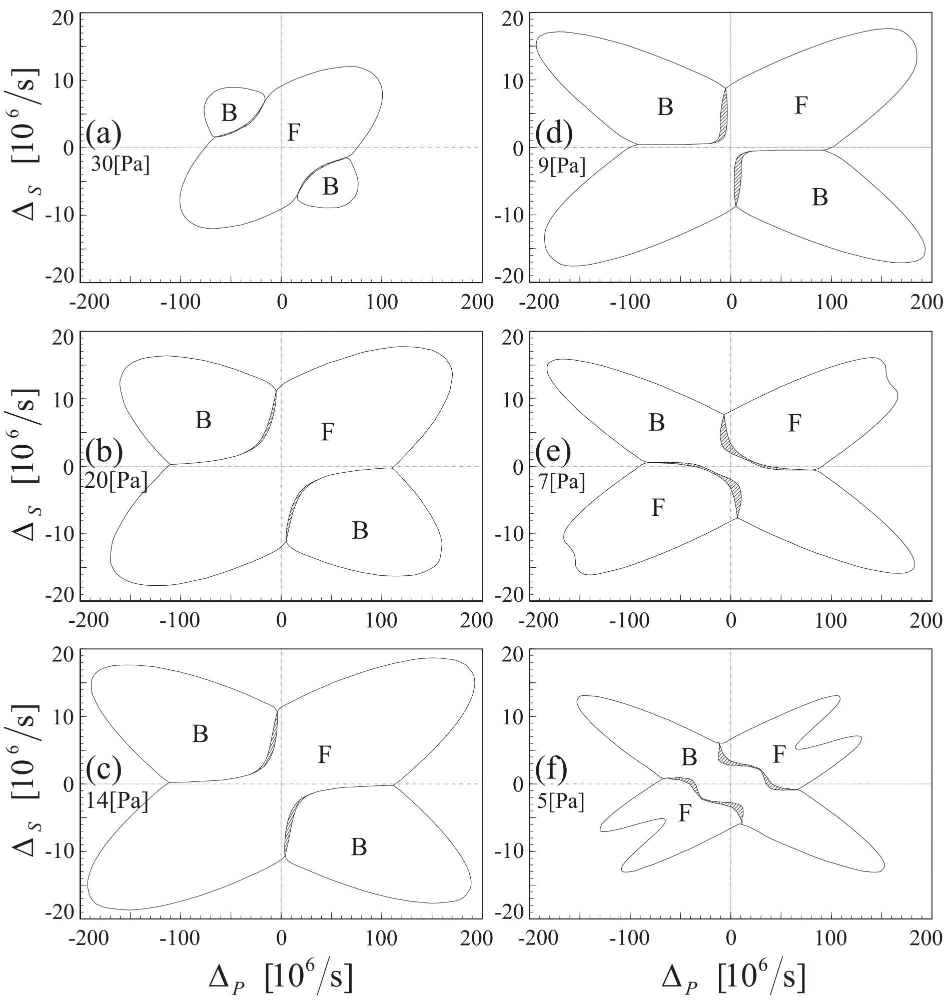

Fig. 5 Calculated threshold contours for different vapor pressures. Pump intensity is 1.7 $\mathrm{W/cm^2}$ and Rabi frequency β of the pump transition is $6.8 \times 10^6\ \mathrm{s^{-1}}$. F: forward unidirectional, B: backward unidirectional, hatched region: bi-directional.

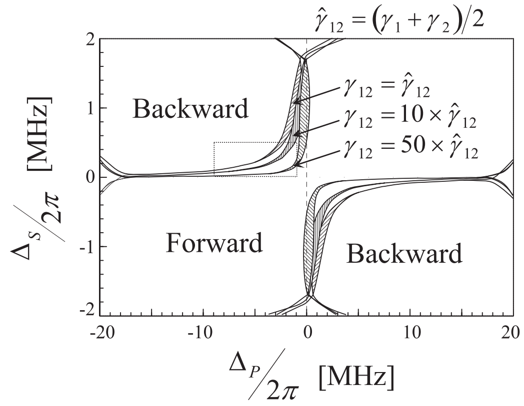

Fig. 6 Calculated threshold contours for different relaxation constants of Raman coherence γ_{12}. The vapor pressure is 14 Pa and the pump intensity is 1.7 $\mathrm{W/cm^2}$. $\hat{\gamma}_{12} = (\gamma_1 + \gamma_2)/2$. The dashed square corresponds to the range in Fig. 3(b). Note that the units of detuning is not same as that in Fig. 5.

of the medium has been neglected in the calculation of the fir Rabi frequencies, the model describes the experimental results shown in Fig. 3.

When the cavity frequency is scanned across the fir line center with the pump detuning being kept fixed, the output direction changes abruptly at a particular cavity frequency. Let's denotes the particular cavity frequency by $\nu_S(\Delta_P)$. On the other hand, the output direction also changes abruptly at particular pump frequency, when the pump frequency is scanned across the pump line center with the cavity detuning being kept fixed. The particular pump frequency is denoted by $\nu_P(\Delta_S)$. For a given negative pump detuning, $|\nu_S(\Delta_P)|$ decreases with a decrease in pressure, as is consistent with the observation shown in Fig. 3(a). The change of output direction does not occur at cavity resonance or at pump resonance. Anisotropic fir gain is responsible for such frequency dependence of direction reversal.

The anisotropic output intensity, as is well known, is caused primarily by Raman-type two-photon process. Threshold contours calculated for different values of the relaxation constant of Raman coherence γ_{12} are plotted in Fig. 6. For a large value of γ_{12}, Raman coherence disappears. Then, the output direction changes at the pump line center or at cavity resonance as the gain becomes isotropic.

The square region in Fig. 6 corresponds to the range in which $\nu_S(\Delta_P)$, i.e. $\nu_R(\Delta_P)$ in Fig. 3(b) has been measured. The observed behavior of $\nu_S(\Delta_P)$ is in qualitative agreement with calculation if we choose so that $\gamma_{12} = 10 \times (\gamma_1 + \gamma_2)/2$.

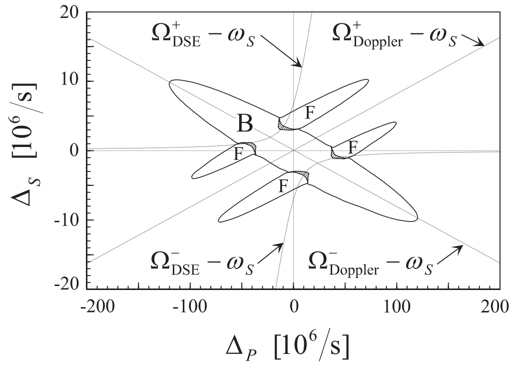

Fig. 7 Threshold contours calculated for vapor pressures of 4 Pa and the pump intensity of 1.7 $\mathrm{W/cm^2}$ (β = $6.8 \times 10^6\ \mathrm{s^{-1}}$). The $\Delta_{\rm DSE}$ and $\Delta_{\rm Doppler}$ are defined in text.

4 Discussion

Forward unidirectional operation of the output prevails on Δ_P-Δ_S plane as shown in Fig. 5(a - c). This is a direct consequence of gain anisotropy due to Raman-type two-photon process in coupled three-level system. Preference of forward output at high pressures has never been predicted in the previous analysis [3] which is based on a mode competition model in rate equation limit ($\gamma_{12} \to \infty$), i.e. two-photon process has been neglected. One of the reasons why we ignored the two-photon process was a small ratio of ω_S/ω_P, i.e. 0.08 for the 119 μm line of $\mathrm{CH_3OH}$. As ratio of forward (G^+) to backward (G^-) gains is approximately given by[8] $G^+/G^- = 1 + \omega_S/\omega_P$, the gain becomes more anisotropic with an increase in ratio ω_S/ω_P. Though the gain anisotropy is as small as 8% for 119 μm line, it significantly affects the output directionality. Such an unexpected influence of the gain anisotropy on the output of OPFRL's is brought about by mode competition between the forward and backward waves in lasing process.

As shown in Fig. 5(e, f), forward output profile splits into two components at low vapor pressures. The splitting is a manifestation of dynamic Stark effect [9]. Resonant frequency of the doublet due to dynamic Stark effect on the pump transition is given by [8]

$$\Omega^{\pm}_{\rm DSE} = \omega_S + \frac{1}{2}\left[\Delta_P \pm \sqrt{\Delta_P^2 + 4\beta^2}\right]. \tag{4}$$

The last term of Eq.(4) plays an important role at low pressures where the homogeneous linewidth becomes smaller than the Rabi frequency of pump transition ($\gamma_{02} < \beta$) [8].

The threshold contour calculated for a vapor pressure of 4 Pa and pump intensity of 1.7 $\mathrm{W/cm^2}$ is shown in Fig. 7. The dashed straight lines are Doppler-shifted resonance frequencies of the fir transition ($\Omega^{\pm}_{\rm Doppler} = \omega_S \pm \Delta_P K_S/K_P$) for the fir waves travelling in the forward ($+$) and the backward ($-$) directions. The dashed curves plot the resonant frequencies of Stark doublet (Eq.(4)).

5 Conclusion

An experimental and theoretical investigation has been made on an optically pumped ring laser which operates on 119 μm line of $\mathrm{CH_3OH}$. For different vapor pressures and pump detunings, we have measured the cavity frequency that gives the change of output direction. The result shows that Raman-type two-photon process makes contribution to the output directionality even if ω_S/ω_P is as small as 0.08.

A closed form of expression of gains for OPFRL model of Doppler broadened 3 level system including two-photon process has been applied to calculation of stable stationary fir intensities in the ring cavity. Threshold contours have been plotted on the parameter plane spanned by cavity and pump detuning. For negative pump detuning, the calculated threshold contours are in qualitative agreement with the experimental results.

The numerical calculation also predicts that at low pressures dynamic Stark splitting modifies the threshold contour of the forward output. At high vapor pressures, the backward output disappears. Then the laser eventually operates unidirectionally and emits only forward output over the whole range of Δ_P and Δ_S.

The anisotropic gain due to two-photon process makes the 119 μm line of $\mathrm{CH_3OH}$ not suitable for an absolute frequency reference [3]. In order to get a change of output direction at fir or ir line center, we prefer the transitions with small Raman-type two-photon transition probability. Cascade fir laser lines and level configuration with a small ω_S/ω_P ratio are the possible candidates for such application.

6 Acknowledgement

We would like to thank Hiroshi Mima for his valuable suggestions and comments, and Noriro Ohashi for his assistance in the computer work.

References

[1] F. Aronowitz and R. J. Collins: Appl. Phys. Lett. **9**, 55(1966).

[2] J. Heppner and C. O. Weiss: Appl. Phys. Lett. **33**, 590(1978).

[3] K. Matsushima, N. Higashida, N. Sokabe and T. Ariyasu: Opt. Commun. **117**, 462(1995).

[4] R. Vilaseca, J.Martorell, R.Corbalan and P. Laguarta: Opt. Commun. **70**, 131(1989).

[5] K. Matsushima, K. Hirata, N. Togawa, N. Sokabe and T. Ariyasu: *Proceedings of Conference on Laser and Electro-Optics* **15**, (1995)43.

[6] K. Matsushima, N. Togawa, Y. Horiuchi and N. Sokabe: *Proceedings of the 19th International Conference on Infrared and Millimeter Waves*, (1994)174.

[7] J. Heppner, C. O. Weiss, U. Hübner and G. Schinn: IEEE J. Quantum Electron. **QE-16**, 392(1980).

[8] D. Seligson, M. Ducloy, J. R. R. Leite, A. Sanchez and M. S. Feld: IEEE J. Quantum Electron. **QE-13**, 468(1977).

[9] A. Javan: Phys. Rev. **107**, 1579(1957).